Thermotropic Polymethacrylate Bearing Sulfonylbenzoxazole-Based Multifunctional Photoactive Mesogen

Sehoon Kim and Soo Young Park*

School of Materials Science and Engineering, Seoul National University, San 56-1, Shillim-dong, Kwanak-ku, Seoul 151-742, Korea

Received December 7, 2000; Revised Manuscript Received March 5, 2001

ABSTRACT: For the multifunctional liquid crystalline medium with high chromophore content, a thermotropic polymethacrylate (PBBS) bearing monolithic photoactive mesogen was designed and synthesized on the basis of semiempirical quantum calculation. PBBS showed phase transition sequence of I−222 °C−SmA−169 °C−SmC−154 °C−SmX on cooling. Phase transition in the PBBS film could be correlated with the birefringence change and H-aggregate formation monitored as a function of temperature. The multifunctional mesogenic pendant, 2-biphenyl-5-sulfonylbenzoxazole, provided strong blue fluorescence and electroluminescence, large second-order optical nonlinearity, and intrinsic photoconductivity to the novel photoactive liquid crystalline polymer PBBS.

Introduction

With profound understanding and easy tunability of π-conjugated nature, molecular materials have been widely exploited for photonic devices such as nonlinear optical (NLO),[1,2] photoconducting,[3] and electroluminescent (EL) devices.[4] Recently, more complicated optoelectronic devices based on the combined activity of different functional chromophores are also attracting great interest. Photorefractivity is a representative example originating from the combination of electrooptic effect and photoconductivity.[5,6]

For most of these molecular optoelectronic devices, not only the electronic properties of photoactive chromophore but also its orientation is an important factor that largely affects the device performance. Among various molecular orientation techniques, cooperative orientation of functional chromophore in liquid crystalline media has been intensively studied due to the effective self-organization and easy processing.[7−9] With conventional nonmesogenic chromophore, however, this method is limited by the inevitable dilution of active chromophore resulting in the reduced device performance. Therefore, use of mesogenic chromophore, i.e., single-component functional liquid crystal, is a better approach for this purpose. For example, low molar mass and polymeric single-component liquid crystals composed of NLO active,[10,11] conductive,[12−14] or fluorescent mesogen[11,15] have already been reported in the literature.

Recently, to make up the complicated photoactive (e.g., photorefractive) medium, great research efforts have been focused on the design and synthesis of a multifunctional molecule, into whose π-conjugated framework several different properties are integrated all together. This approach has successfully been applied to the multifunctional single-component organic glass as a new property-combining strategy,[16] but few studies have been carried out for the single-component multifunctional liquid crystal.[11] Chart 1 shows the chemical structure of potentially mesogenic, multifunctional photoactive chromophore designed in this work along this concept. Basically, the central π-conjugated bridge, composed of biphenyl and benzoxazole groups, is fully aromatic and anisotropic in shape with a large aspect ratio. The benzoxazole moiety, a thermally and optically stable fused heteroaromatic ring, is included to provide efficient fluorescence[17] and photoconductivity.[12,13] Alkoxy and sulfonyl groups substituted at either end of mesogenic structure are intended to induce intramolecularly charge-separable dipolar character responsible for second-order optical nonlinearity.[1,2] Thus, photorefractivity is also expected for this simple multifunctional liquid crystalline medium as a combination of the latter two properties.

Chart 1. Multifunctional Mesogenic Chromophore

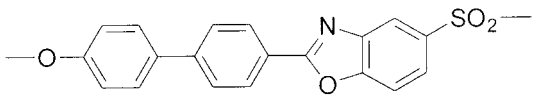

In this work, we report the synthesis and properties of a liquid crystalline polymethacrylate bearing this multifunctional photoactive mesogen. In particular, mesomorphic behavior and applicability of the polymer film have been investigated.

Experimental Section

Measurements. Chemical structures were identified by ^{1}H NMR (JEOL JNM-LA300, 300 MHz) and mass spectroscopy (JMS AX505WA). Thermal analysis was performed on Perkin-Elmer DSC7 and TGA7 at a rate of 10 °C/min. A polarizing optical micrograph (POM) was obtained using Leica DMLP equipped with a heating stage controlled by a Eurotherm controller. Highly resolved wide-angle X-ray scattering (WAXS) was recorded with a 1-dimensional diode array detector utilizing the monochromated light (1.608 Å) from a synchrotron at the Pohang Accelerator Laboratory (4C1 line).

The UV−vis absorption spectrum was recorded with a HP 8452A diode array spectrophotometer. Photoluminescence (PL) and electroluminescence (EL) emission spectra were obtained using an ISS PL1 fluorometer with a 300 W xenon arc lamp. For hyper-Rayleigh scattering (HRS) and second harmonic generation (SHG) measurements, a 1064 nm Nd:YAG laser (10 Hz, 3−8 ns pulse width) was used as a fundamental radiation. The HRS measurement was performed in chloroform at room temperature, following the literature method.[18] For the SHG measurement, a standard corona poling technique

* Corresponding author: E-mail parksy@plaza.snu.ac.kr.

10.1021/ma002087e CCC: $20.00
Published on Web 05/08/2001

Chart 2. Low Molar Mass Benzoxazole Compounds

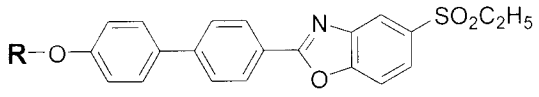

HBBS : **R**=hexyl

MBBS : **R**=6-methacryloyloxyhexyl

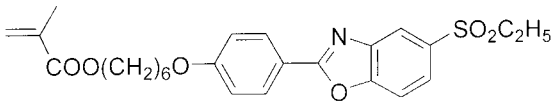

MPBS

was used in a wire-to-plane geometry (7 kV) at increasing temperature. The SHG coefficient d_{33} was determined by the standard Maker fringe technique in p−p configuration using a quartz crystal reference. To measure the first ionization potential of polymer, cyclic voltametry was carried out for polymer film coated on an indium tin oxide (ITO) electrode in 0.1 M acetonitrile solution of tetrabutylammonium tetrafluoroborate at a rate of 20 mV/s using three electrode cells and a potentiostat assembly (model 362, EG&G Princeton Applied Research). The obtained oxidation potential of the polymer film was calibrated using ferrocene as a reference whose ionization potential is −4.8 eV with respect to zero vacuum level. Photocurrent was measured by an electrometer (Keithly 6517A) with illumination of light from a xenon arc lamp (290 W) filtered by a band-pass filter (Coherent 35-2989-000, 340 nm). For various film state measurements, PBBS films of the desired thickness were prepared by spin-casting from the 1,1,2,2-tetrachloroethane solution of an appropriate concentration (2−10 wt %) filtered by a 0.5 μm syringe filter.

Semiempirical Calculation Method. Following the literature method,[19] we employed the PM3 procedure to optimize the ground-state geometry and predicted the first hyperpolarizability (β_0) based on the time-dependent Hartree−Fock (TDHF) approach, implemented in the Mopac 97 program (Fujitsu Limited). For the simplicity, the alkoxy substituent, attached at the biphenyl side, was set to ethoxy. The one-electron excitation energies and the corresponding oscillator strengths as well as transition dipole moments between singlet states were calculated for the optimized geometry by considering the configuration interaction (CI) with 61 configurations, utilizing the HyperChem 5.0 program (Hypercube, Inc.).

Synthesis of Sulfonylbenzoxazole Derivatives. Low molar mass benzoxazole compounds with sulfonyl end groups, studied in this work, are shown in Chart 2. The synthetic procedure for HBBS was reported in the previous work.[20] Methacrylate monomer MBBS was prepared by two different methods. The one is the same procedure as that for HBBS (method A, vide infra), and the other is a simplified method (method B, vide infra). Phenyl-analogous benzoxazole monomer MPBS was prepared to examine the effect of mesogenic shape anisotropy, that is, the aspect ratio of mesogen. Its synthetic procedure followed the similar method as described previously, i.e., direct cyclization between 4-hydroxybenzaldehyde and 2-amino-4-(ethylsulfonyl)phenol in the presence of lead(IV) acetate, followed by the introduction of alkoxy spacer and vinyl group.[21] In the text below, synthesis of MBBS and its polymerization are described in detail.

4′-(6-Hydroxyhexyloxy)biphenyl-4-carboxylic Acid (1). To a refluxed mixture of 4.6 g of 4′-hydroxybiphenyl-4-carboxylic acid (21.5 mmol), 10 g of KOH, and 0.5 g of KI in 60 mL of ethanol was added 40 mL of 6-chlorohexan-1-ol in 40 mL of ethanol slowly. After the vigorous stirring for 2 days, 5 g of KOH was added to the mixture, followed by additional reflux for 1 day. After cooling, the mixture was poured into cold water and acidified with 2 N HCl solution. The precipitate was filtered and washed several times with water, affording 6.5 g of a white solid (**1**). This crude product was pure as judged by thin-layer chromatography (TLC): 96% yield.

4′-[6-(2-Methacryloyloxy)hexyloxy]biphenyl-4-carboxylic Acid (3). To a mixture of 6 g of **1** and 5.5 mL of triethylamine in 100 mL of 1,4-dioxane was added 6 mL of methacryloyl chloride slowly in ice bath. The mixture was stirred overnight at room temperature and poured into cold water. The product was extracted using ethyl acetate, and the extract was dried with anhydrous $MgSO_4$. After removal of solvent, the resultant solid (**2**) was dissolved in 100 mL of glacial acetic acid. This solution was gently boiled for 30 min, cooled, and poured into cold water. The precipitate was filtered, washed several times with water, and recrystallized from ethanol, affording 5 g of a white solid (**3**): 69% yield. ^{1}H NMR (DMSO-d_6, ppm): 1.26−1.74 (m, 8H), 1.88 (s, 3H), 4.02 (t, J = 6.3 Hz, 2H), 4.11 (t, J = 6.5 Hz, 2H), 5.66 (s, 1H), 6.02 (s, 1H), 7.04 (d, J = 8.2 Hz, 2H), 7.68 (d, J = 8.2 Hz, 2H), 7.75 (d, J = 8.3 Hz, 2H), 7.99 (d, J = 8.3 Hz, 2H).

Methacrylate Monomer (MBBS): Method A. A 3 g sample of **3** was dissolved in 5 mL of thionyl chloride containing 1 drop of *N*,*N*-dimethylformamide. After the reflux for 1 h, thionyl chloride was removed under reduced pressure. The residual acid chloride (**4**) was dissolved in 60 mL of 2:1 (by volume) CCl_4/tetrahydrofuran (THF) and was added slowly to a mixture of 2.4 g of 2-amino-4-(ethyl-sulfonyl)phenol and 1.5 mL of triethylamine in 100 mL of 9:1 CCl_4/THF in ice bath. The reaction mixture was stirred overnight at room temperature and poured into cold water. After extraction using $CHCl_3$, the extract was washed with water and dried with anhydrous $MgSO_4$. Solvent was evaporated, and the residual solid was recrystallized from ethanol to give *o*-(acylamino)phenol (**5**). The solution of **5** in 5 mL of *o*-dichlorobenzene containing catalytic amount of *p*-toluenesulfonic acid was heated at 130 °C for 3 h. The cooled reaction mixture was poured into water and extracted with $CHCl_3$. After washing and drying the extract, the solvent was evaporated, and the crude product was purified by silica gel column chromatography with the eluent ethyl acetate/*n*-hexane (the volume ratio increasing from 1/2 to 2/1). The obtained white solid was further purified by recrystallization from $CHCl_3$/ethanol (4:1), affording 2 g of 2-methacrylic acid 6-[4′-(5-ethanesulfonylbenzoxazol-2-yl)biphenyl-4-yloxy]-hexyl ester (MBBS): 47% yield. ^{1}H NMR ($CDCl_3$, ppm): 1.30−1.87 (m, 11H), 1.95 (s, 3H), 3.19 (q, J = 7.5 Hz, 2H), 4.03 (t, J = 6.34 Hz, 2H), 4.17 (t, J = 6.6 Hz, 2H), 5.55 (s, 1H), 6.10 (s, 1H), 7.01 (d, J = 8.8 Hz, 2H), 7.61 (d, J = 8.8 Hz, 2H), 7.74−7.77 (m, 3H), 7.94 (dd, J = 8.4, 1.8 Hz, 1H), 8.30−8.34 (m, 3H); m/z (EI) calcd for $C_{31}H_{33}NO_6S$, 547.66; found 547.

Method B. The acid chloride (**4**) dissolved in NMP was dripped into a solution of the equivalent 2-amino-4-(ethylsulfonyl)phenol in NMP at room temperature under N_2. After addition was complete, the temperature was increased to 160 °C for 12 h. The cooled reaction mixture was poured into excess of water. The final product MBBS was isolated from the filtered precipitate by the same procedure described in method A: 56% yield.

Polymerization of MBBS (PBBS). The solution of 0.4 g of MBBS and 1.2 mg of AIBN in 4 mL of NMP, sealed in an ampule, was heated to 65 °C and kept for 60 h. After cooling, the solution was poured into methanol. The white precipitate was filtered and purified by Soxhlet apparatus using hot methanol, to give 0.33 g of PBBS: 83% conversion.

Results and Discussion

Synthesis and Thermal Properties. Two synthetic methods for methacrylate monomer MBBS are depicted in Scheme 1. Method A is a general procedure for benzoxazole synthesis consisting of two separate successive steps, i.e., kinetically controlled amidation and acid-catalyzed dehydrative ring closure of the obtained *o*-(acylamino)phenol. Method B is a simply modified version of method A, i.e., thermodynamically controlled one-step reaction between carboxylic acid chloride (**4**) and *o*-aminophenol at high temperature. In addition to

Scheme 1. Synthesis of Methacrylate Monomer MBBS

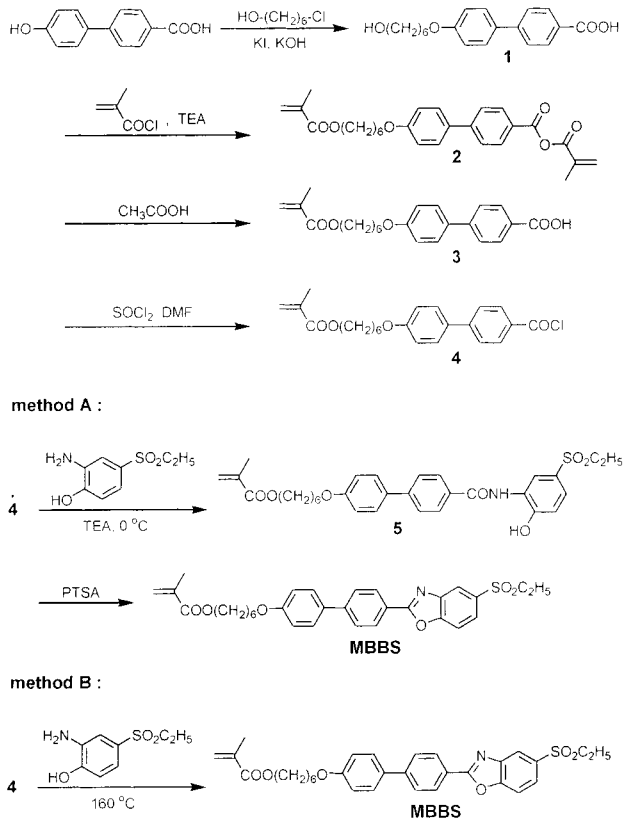

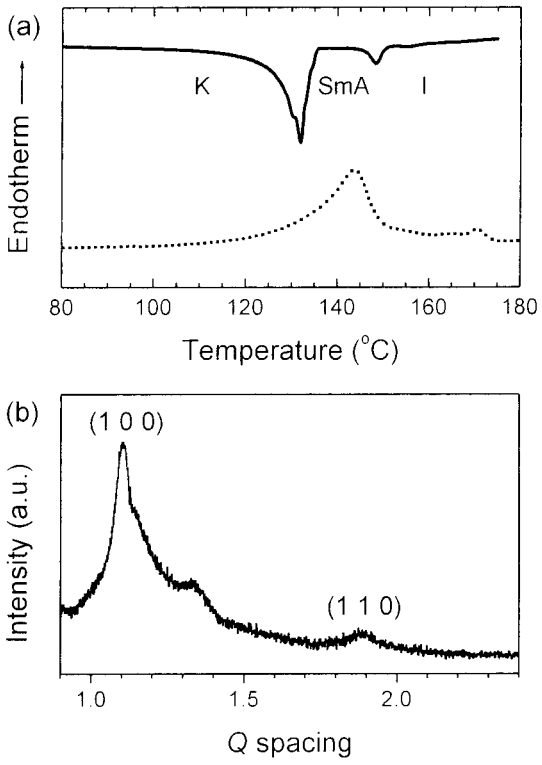

Figure 1. (a) DSC thermogram of MBBS: the first cooling (straight) and the second heating (dotted) runs. (b) Wide-angle X-ray scattering (WAXS) intensity curve of PBBS.

the favorable simplicity of one-step procedure, method B showed better yield (56%) than method A (47%). Methacrylate homopolymers, PBBS and PPBS, were prepared by free radical polymerization of MBBS and MPBS, respectively. ^{1}H NMR spectra of polymers showed characteristic line broadening feature and no vinyl proton peaks at 5.5−6.1 ppm. From the gel permeation chromatography (GPC) experiment, the number-average molecular weight (M_n) was estimated as 15 600 (M_w/M_n = 1.65) for PBBS and 10 700 (M_w/M_n = 1.58) for PPBS. PBBS is soluble in 1,1,2,2-tetrachloroethane, chloroform, and NMP but partly soluble in 1,2-dichloroethane, and rarely in THF, whereas PPBS is sufficiently soluble in common organic solvents.

Thermal properties of the synthesized sulfonyl-containing benzoxazoles showed significant dependence on the mesogen length and the flexible chain. In the previous work, it has been found that HBBS is only crystalline with melting point (T_m) at 193 °C.[20] On the contrary, MBBS exhibits mesophase with a help of extended flexible chain (Figure 1a). In the range between the crystalline (K) and isotropic (I) melting peaks, MBBS showed a fan-shaped texture between the crossed polarizers, indicative of the smectic A (SmA) phase. Meanwhile, a short mesogen, 2-phenylbenzoxazole, was found to be insufficient in length for sulfonyl-substituted benzoxazole to induce mesophase. MPBS is only crystalline with T_m at about 60 °C, and the corresponding homopolymer PPBS is amorphous with a glass transition temperature (T_g) at 73 °C. This tendency is consistent with the report that in the case of sulfonyl-containing liquid crystals the presence of mesophase was strongly dependent on the mesogen length due to the strong dispersion force of sulfur atom.[22]

The thermal properties of PBBS[23] investigated with DSC, WAXS, POM, and thermogravimetry analysis (TGA) are summarized as follows: (1) the pristine PBBS powder formed by precipitation from solution is partly amorphous and exhibited partial recrystallization (90−110 °C) and glass transition (160 °C) on heating; (2) after the first heating, PBBS showed reversible phase transition sequence without noticeable T_g, that is, ordered smectic phase (SmX)−179 °C−SmA−230 °C−I on heating and I−222 °C−SmA−169 °C−SmC−154 °C−SmX on cooling; (3) the mesogen tilt angle in SmX phase is 25°; and (4) the degradation temperature corresponding to a 5% weight loss was 393 °C, demonstrating excellent thermal stability of the benzoxazole mesogen. In SmX, the X-ray powder diffraction pattern showed a noticeably narrowed halo in the wide-angle region. The highly resolved diffraction pattern of preannealed PBBS powder in the wide-angle region, which was recorded at room temperature using high-intensity X-ray from synchrotron, shows a main peak (5.7 Å) and a higher-order diffraction peak (3.3 Å), as shown in Figure 1b. From their reciprocal Q ratio of 1:$\sqrt{3}$, these two peaks are assignable to (100) and (110) reflections in hexagonal array. Therefore, it is concluded that the positional long-range order was developed to some extent within the layer and that PBBS exists in ordered smectic phase in the low-temperature range with hexagonal order and tilt orientation, similar to SmF or SmI.

Electronic Properties of Chromophore. Figure 2 shows the schematic diagram of the highest occupied molecular orbital (HOMO) and the lowest unoccupied molecular orbital (LUMO) of our multifunctional mesogenic chromophore, obtained by semiempirical quantum calculation. As can be seen in the diagram, HOMO has aromatic character while LUMO has quinoid character. This feature strongly suggests that the excited-state intramolecular charge transfer through conjugated π-framework from electron donor (alkoxy) to acceptor (sulfonyl) is efficient, which plays a crucial role within

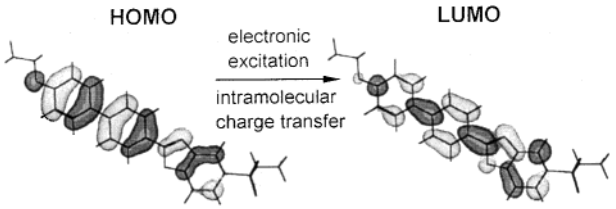

Figure 2. Sketches of HOMO and LUMO diagrams of the designed chromophore.

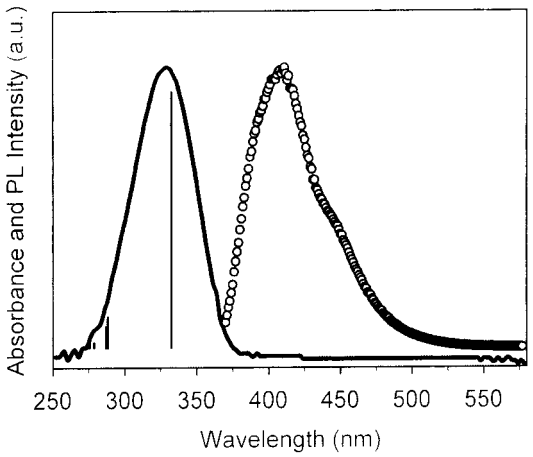

Figure 3. Absorption (straight) and photoluminescence (open circle) spectra, excited at 320 nm, of MBBS in chloroform ($\sim 10^{-5}$ M). Vertical bars in the absorption spectrum indicate the calculated transition energies and oscillator strengths for the structure in Figure 2.

the perturbation theory for the molecular second-order nonlinearity.[1,2] Actually, the nonresonant first hyperpolarizability (β_0) was calculated as 22.6×10^{-30} esu by the TDHF method and experimentally determined to be 56×10^{-30} esu for MBBS by the HRS technique. The difference between these two values may be due to the different conformations and the different electronic state levels in solution (HRS) and isolated gas phase (calculation), which has already been discussed in our previous publication.[24] By any means, it can be concluded that the designed chromophore has a distinct photoactivity toward the nonlinear optical applications.

The orbital diagram in Figure 2 also indicates another significant point that S_0 may be very stable due to aromatic stabilization while S_1 is very unstable due to the breakage of aromaticity, implying a large energy gap. Moreover, it is well-known that sulfonyl group shows less bathochromic effect than conventional electron acceptors such as nitro and polycyanovinyl groups.[1] Thus, it is expected that the fully aromatic character of the target chromophore and the presence of sulfonyl group would provide the possibility of visible region transparency and blue emission. The calculated HOMO-to-LUMO transition energy, which was estimated as 332 nm, supports this prediction quantitatively. Actually, MBBS exhibited large absorption energy ($\lambda_{max,abs} = 328$ nm) and blue emission ($\lambda_{max,PL} = 410$ nm), consistent with the theoretical prediction (Figure 3). The direction of the transition dipole moment, i.e., the optical axis, was calculated to be almost parallel to the molecular long axis defined geometrically from oxygen atom of donor to sulfur atom of acceptor at an angle of 2°, well supporting the intramolecular charge-transfer feature. Moreover, to our interest, MBBS emitted a very strong fluorescence. In our previous work, the absolute photoluminescence (PL) quantum efficiency of dilute chloroform solution of HBBS was measured as 0.9 when excited at the absorption λ_{max}.[20] The relative PL quantum efficiency of MBBS, which was determined using HBBS as a reference following the literature method,[25] was also the same value owing to the same chromophore unit. The nitro group, a conventional acceptor in NLO chromophores, is known to quench fluorescence due to a rapid dissipation of the electronic energy.[26] However, as was shown in our case, the sulfonyl group does not have this kind of quenching effect and has been adopted in this work as an electron-withdrawing substituent for single- or multiphoton-absorbing fluorophore. Thus, it can be concluded that the sulfonyl group plays a major role for the aforementioned multifunctionality, i.e., significant second-order nonlinearity and intense blue fluorescence as well as visible region transparency.

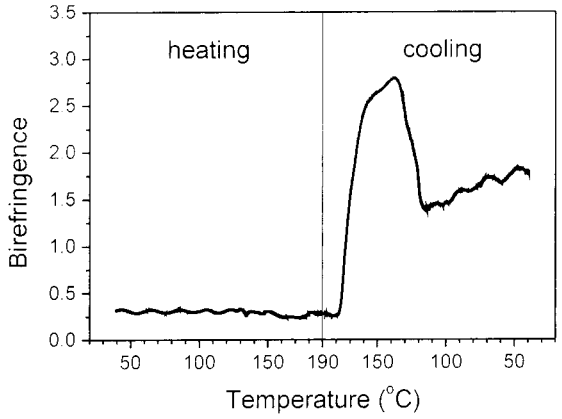

Figure 4. Birefringence change in the as-spun PBBS film at 633 nm (He−Ne laser).

Film Properties of PBBS. When spin-cast from tetrachloroethane solution, thermotropic homopolymer PBBS forms metastable amorphous clear film by rapid evaporation of solvent. On heating, the transparency was maintained up to 300 °C, but on cooling, the PBBS film became hazy and birefringent. This film state morphological behavior as a function of temperature was monitored by the birefringence change between the crossed polarizers at 633 nm where the absorption of PBBS film is ignorable. Figure 4 shows the birefringence change with the temperature variation at 10 °C/min. The as-spun film shows small but nonzero birefringence at room temperature even before annealing. When heated to 190 °C, no noticeable change in birefringence was observed. This temperature corresponds to the SmA phase, and the partly amorphous PBBS may experience the following thermal processes: (1) recrystallization from metastable amorphous state to SmX phase, (2) transition from SmX phase to SmA phase, and (3) development of SmA domain. However, the absence of the increase in birefringence in the first heating run means that these processes may be severely depressed in the film state by a large surface interaction between the substrate and the polymer film and thus that amorphous state remains up to 190 °C at the heating rate of 10 °C/min. On the other hand, on cooling at the same rate, birefringence dramatically increased, indicative of the transition from metastable amorphous state to the thermodynamically stable SmX phase. This feature can be supported by the large enthalpy change ($\Delta H = 16$ J/g) of the transition to SmX in cooling run. The decrease in birefringence below 137 °C can be understood as transmission loss of the incident light by scattering on the hazed film.

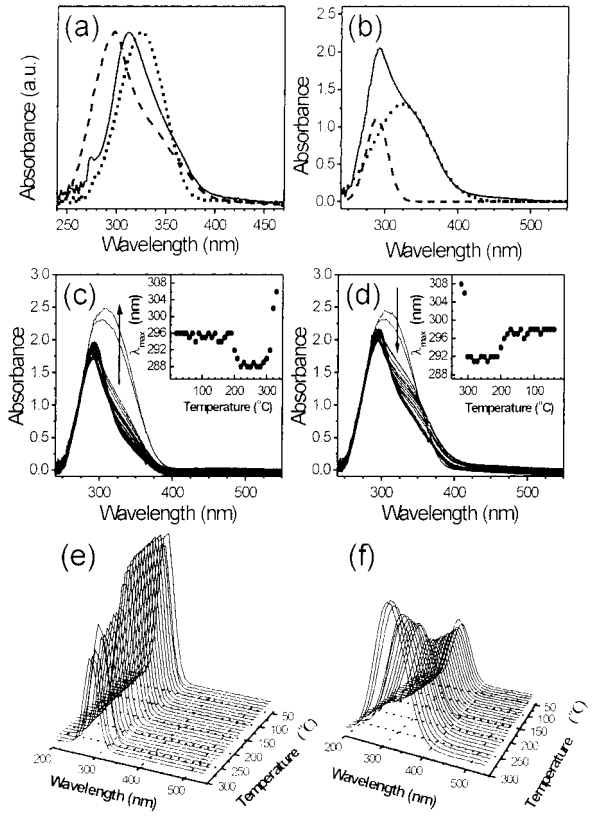

Figure 5. Absorption behavior of PBBS: (a) normalized absorption spectra of the chloroform solution (dotted), the as-spun (straight), and the annealed (dashed) films, (b) peak separation of the annealed film absorption spectrum by Gaussian curve fitting. (c) and (d) are heating and cooling traces of absorption in film state, respectively (the insets indicate the temperature traces of λ_{max}). (e) and (f) show the temperature-dependent intensity changes of H-aggregate and monomer absorptions, separated from (d) by Gaussian curve fitting.

Figure 5a shows the absorption spectra of the dilute chloroform solution, the as-spun film, and its annealed film of PBBS. The absorption spectrum of PBBS solution is almost the same as that of monomer MBBS in solution, whereas that of the as-spun film exhibited a blue shift of band maximum by 13 nm. This spectral change and the aforementioned nonzero birefringence of the as-spun film indicate that partial stacking of mesogen exists in metastable amorphous state. After annealing, the band maximum was blue-shifted by 14 nm, and a shoulder on the long-wavelength side became noticeable, as compared with that of the as-spun film. This spectral change may arise from the further stacking, i.e., orientational ordering of the conjugated mesogens within multidomains by annealing. According to the molecular exciton model proposed by Kasha et al., a blue shift of the absorption maximum is indicative of H-aggregation of linear chromophores.[27] Moreover, the mesogen tilt angle of 25° in the annealed PBBS film at room temperature, which was determined from the WAXS result, satisfies the H-aggregate forming angle range. Thus, it is appropriate to mention that the annealed PBBS film would exhibit H-type aggregation behavior. On the basis of this consideration, the absorption spectrum of the annealed film can be figured out as the sum of two Gaussian curves, as shown in Figure 5b: the blue band (dashed) is assignable to H-aggregate absorption and the red one (dotted) to monomer absorption. Actually, the red-band absorption matches well

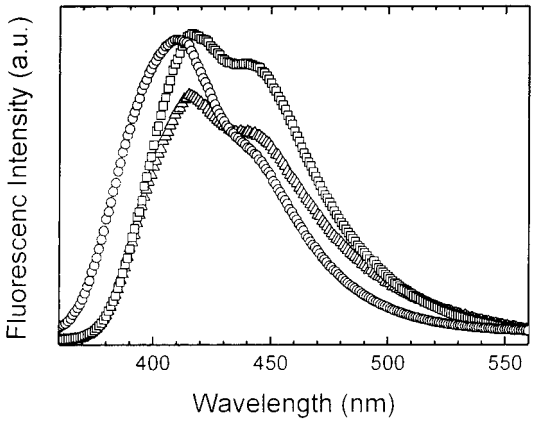

Figure 6. Photoluminescence spectra of PBBS: the chloroform solution (circle), the as-spun (rectangle), and the annealed (triangle) films, each excited at absorption λ_{max}.

with the monomer MBBS solution absorption in Figure 3. The temperature dependence of the PBBS film absorption showed reversible spectral changes on the second and subsequent heating and cooling runs at 10 °C/min by the step of 10 °C, as shown in Figure 5c,d. Above 300 °C, the absorption curve becomes broad and intense with Gaussian shape, indicative of isotropic melting, i.e., random orientation of mobile chromophores, whereas below 300 °C the spectra exhibit H-aggregation feature similar to Figure 5b. To monitor the phase-dependent hypsochromic effect of H-aggregation, the absorption band maxima were plotted against temperature in the insets of Figure 5c,d. It is clearly seen that the band maximum changes slightly but discontinuously at phase transition temperatures. As shown in the inset of Figure 5d, on cooling from isotropic phase, an abrupt blue shift was observed at 300 °C, indicative of H-aggregate formation in SmA phase. On going from SmA to the SmX, the band maximum slightly red-shifted at around 190 °C; that is, the hypsochromic effect decreased as compared with that in SmA phase. This sequence of band maximum proceeded reversibly on heating, as shown in the inset of Figure 5c, implying the reversible phase transition of PBBS film. It is well-known that the hypsochromic shift due to H-aggregation is more effective with the more parallel stacking of chromophores.[27] Therefore, it can be deduced that the hypsochromic effect would be more pronounced in orthogonal smectic phase than in tilted one and thus that the reduced hypsochromic shift below 190 °C is attributable to the tilted array of mesogens in the SmX phase of PBBS. Figure 5e,f shows the cooling traces of H-aggregate and monomer absorption intensities. It can be clearly seen that H-aggregate contribution jumps up and monomer contribution down upon the transition from SmA to SmX, which is probably due to the development of long-range order within the smectic layer and the reduced intermesogenic distance.

Figure 6 shows the fluorescence spectra of PBBS. The fluorescence of PBBS in good solvent (chloroform, $\sim 10^{-5}$ M) showed almost the same spectral characteristics as that of monomer MBBS solution in Figure 3: a main band at 410 nm and a shoulder at around 440 nm. The fluorescence efficiency of PBBS solution was measured as rather lower value of 0.86 than that of MBBS, probably due to the intermolecular proximity between mesogenic side chains of homopolymer. The PBBS films also showed the monomer-like fluorescence spectral features. In the as-spun state and even in the annealed

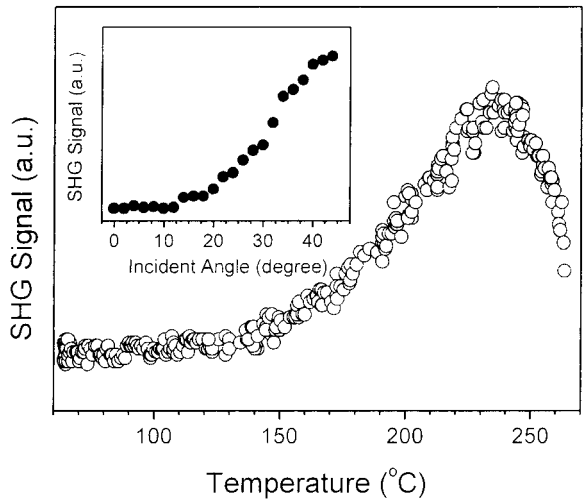

Figure 7. Temperature dependence of SHG signal in the as-spun PBBS film. The inset is Maker fringe curve of the as-spun PBBS film, obtained at room temperature.

state, no discernible excimer emission was observed except for a slight shift of the main band to 416 nm and the increased intensity ratio of the shoulder to the band. Moreover, it is notable that the as-spun film emits very intense fluorescence comparable to that of the PBBS solution with the relative fluorescence efficiency of ca. 0.8, while that of the annealed film was reduced to ca. 0.5. The H-aggregate absorption and the monomer-like fluorescence of the annealed PBBS film are well consistent with the behavior of cyanooctyloxybiphenyl in its neat form of smectic-like crystalline phase reported by Itaya et al.[28] The monomer-like fluorescence without excimer emission, emitted from the annealed PBBS film in SmX phase, can be interpreted due to the rigid molecular arrangement. Excimer formation is a bimolecular process between the ground- and excited-state molecules within ca. 4 Å.[29] In the liquid crystalline phase with a larger intermolecular distance, such an bimolecular association is reported to be possible due to the molecular mobility.[30] In the crystal-like SmX phase of PBBS, however, the intermesogenic distance within the smectic layer is estimated as ca. 6.6 Å from WAXS, and the molecular arrangement is so rigid that an excimer formation might be hindered, only affording the monomer-like fluorescence.

Second Harmonic Generation (SHG) in the As-Spun Film. Though the side chain of PBBS has molecular second-order nonlinearity as discussed above with its molecular hyperpolarizability β, the as-spun PBBS film would have no second-order NLO property due to the cancellation of dipole moment by random orientation. To study the bulk NLO property in the film state, a preliminary experiment on SHG imparted by corona poling was carried out at the fundamental wavelength of 1064 nm. An interesting point in the PBBS film is that corona discharge generates a detectable second harmonic signal even at room temperature where the molecular motion is frozen by kinetic constraints. The SHG signal exhibited a rise followed by saturation in the presence of the field and a subtle relaxation in the absence of the field. The inset of Figure 7 shows a Maker fringe curve of the as-spun film (0.7 μm thick) obtained after corona poling (7 kV) at room temperature, from which SHG coefficient d_{33} was estimated as ca. 3 pm/V. This value of d_{33} is rather small but is essentially a nonresonant value since the absorption of PBBS at the harmonic wavelength (532 nm) is negligible. This peculiar behavior far below T_g is not a common case in conventional NLO polymers, and the origin can be found in the liquid crystallinity of PBBS. Just after spinning, the PBBS film exists in the metastable amorphous state, which means that the external stimulation (e.g., heat, electric field, mechanical stress) may induce the morphological change toward the thermodynamically favored SmX phase. In the present study, SHG at room temperature is evidence of a morphological change induced by electrical stimulus. The dipolar mesogens of PBBS with positive dielectric anisotropy ($\Delta\epsilon = \epsilon_{\parallel} - \epsilon_{\perp}$) would tend to align with their long axes parallel to the poling field. Therefore, the small value of d_{33} at room temperature implies that, in the presence of the electric field, noncentrosymmetry arising from the axial orientation was presumably developed not fully but to some extent surmounting the kinetic constraints in the frozen glassy state.

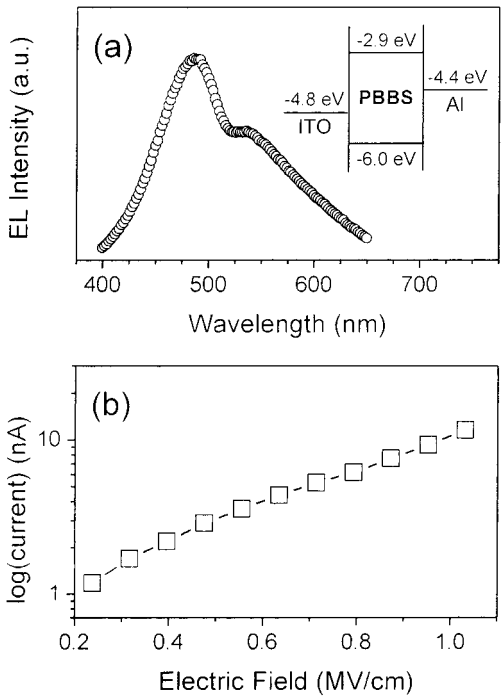

Figure 8. (a) Electroluminescence spectrum and energy levels of PBBS single layer device. (b) Electric field dependence of photocurrent in PBBS film.

The temperature dependence of SHG signal with increasing temperature is shown in Figure 7. Up to ca. 150 °C, only a subtle increase of the signal was observed, indicating the hindered molecular motion in the field-induced SmX phase. A remarkable increase in the signal appeared just above this temperature, indicating the transition to the SmA phase with enhanced polymer mobility. A sudden decrease around ca. 240 °C indicates the onset of isotropic phase, where the thermally random motion of mesogen would surmount the electric field coupled motion.

Electroluminescent (EL) and Photoconducting Properties. Motivated by the strong fluorescence of PBBS film, a single-layer device of Al/PBBS (ca. 90 nm)/ITO was fabricated in order to test the applicability to electroluminescence device. Figure 8a shows the energy levels involved in the device and the EL spectrum obtained at 18 V, where the broadened and red-shifted spectral characteristics were observed with respect to PL. The emission was as strong as to be seen clearly by

the naked eye under room light. However, this device exhibited poor conducting behavior under the applied electric field and thus large Joule heat, resulting in an early breakdown. The device instability can be understood with a help of energy levels, where the HOMO level and the band gap (E_g) were determined from the first ionization potential obtained by cyclic voltametry (CV) and the edge of absorption spectrum, respectively. Since the carrier injection barriers are quite large on both sides of electrodes due to a large E_g (=3.1 eV), PBBS film would tend to behave as a capacitor rather than a conductor until high voltage, which might give rise to the poling effect as was revealed in SHG behavior. The field-parallel orientation of the mesogens may further increase the resistivity due to the lower carrier mobility along the normal direction of the smectic layer. This conducting limitation can be overcome by an appropriate fabrication of the multilayer EL device. By any means, the luminescence from the current coarse device suggests that PBBS is a promising blue emitter for EL application, including linearly polarized luminescence with homogeneously monodomain alignment.[15]

In addition to the PL and EL characteristics, photoconductivity is another potential functionality arising from full conjugation and fused heteroaromaticity of PBBS mesogen. The intrinsic photoconductivity has already been reported for the similar structure, 2-(4′-heptyloxyphenyl)-6-dodecylthiobenzothiazole.[12,13] Figure 8b shows the photocurrent of the preannealed PBBS film illuminated with mild intensity light filtered at 340 nm, where no texture change was observed in the applied field range. Although the photocarrier generation quantum yields in "pure" UV-absorbing photoconductors are usually low, a typical field dependence of photocurrent was clearly observed in PBBS film without any sensitizer, indicating that the intrinsic photocarrier generation in PBBS film can be interpreted by Onsager theory.[3] This finding strongly suggests that PBBS is a photoconductor itself possessing photocarrier generation ability as well as carrier transportability.

Conclusions

2-Biphenyl-5-sulfonylbenzoxazole, the mesogen of PBBS, was proven to be a truly monolithic and multifunctional chromophore, possessing optical nonlinearity, fluorescence, and photoconductivity within a single π-framework. The combination of these properties in a single-component liquid crystalline medium would open new technological applications in molecular materials science.

Acknowledgment. This research was supported by CRM-KOSEF (1999). We are grateful to Prof. B. R. Cho, Department of Chemistry, Korea University, for HRS experiment, and Dr. J. K. Kim, Polymer Materials Laboratory, Korea Institute of Science and Technology, for CV, PL, and EL measurements.

References and Notes

(1) *Materials for Nonlinear Optics: Chemical Perspective*; Marder, S. R., Sohn, J. E., Stucky, G. D., Eds.; ACS Symposium Series 455; American Chemical Society: Washington, DC, 1991.
(2) Zyss, J. *Molecular Nonlinear Optics*; Academic Press: New York, 1994.
(3) Law, K.-Y. In *Organic Conductive Molecules and Polymers;* Nalwa, H. S., Ed.; John Wiley & Sons Ltd.: West Sussex, 1997; Vol. 1, p 487.
(4) *Organic Light-Emitting Materials and Devices*; Hsieh, B. R., Ed.; Macromol. Symp. 125; Hüthig & Wepf Verlag, Zug: Oxford, 1997.
(5) Moerner, W. E.; Silence, S. M. *Chem. Rev.* **1994**, *94*, 127.
(6) Moerner, W. E.; Grunnet-Jepsen, A.; Thompson, C. L. *Annu. Rev. Mater. Sci.* **1997**, *27*, 585.
(7) Trollsås, M.; Sahlén, F.; Gedde, U. W.; Hult, A. Hermann, D.; Rudquist, P.; Komitov, L.; Lagerwall, S. T.; Stebler, B.; Lindström, J.; Rydlund, O. *Macromolecules* **1996**, *29*, 2590.
(8) Kato, M.; Ohara, H.; Fukuda, T.; Matsuda, H.; Nakanishi, H. *Macromol. Chem. Phys.* **1998**, *199*, 881.
(9) Stumpe, J.; Läsker, L.; Fischer, Th.; Rutloh, M.; Kostromin, S.; Ruhmann, R. *Thin Solid Films* **1996**, *284*−*285*, 252.
(10) Barbera, J.; Giménez, R.; Serrano, J. L.; Alcala, R.; Villacampa, B.; Villalba, J.; Ledoux, I.; Zyss, J. *Liq. Cryst.* **1997**, *22*, 265.
(11) Barberá, J.; Clays, K.; Giménez, R.; Houbrechts, S.; Persoons, A.; Serrano, J. L. *J. Mater. Chem.* **1998**, *8*, 1725.
(12) Funahashi, M.; Hanna, J. I. *Jpn. J. Appl. Phys., Part 2* **1996**, *35*, L703.
(13) Funahashi, M.; Hanna, J. I. *Phys. Rev. Lett.* **1997**, *78*, 2184.
(14) Tokuhisa, H.; Era, M.; Tsutsui, T. *Appl. Phys. Lett.* **1998**, *72*, 2639.
(15) Grell, M.; Bradley, D. D. C. *Adv. Mater.* **1999**, *11*, 895.
(16) Sohn, J.; Hwang, J.; Park, S. Y.; Lee, J.-K.; Lee, J.-H.; Jang, J.-S.; Lee, G. J.; Zhang, B.; Gong, Q. *Appl. Phys. Lett.* **2000**, *77*, 1422.
(17) Krasovitskii, B. M.; Bolotin, B. M. *Organic Luminescent Materials*; VCH: Weinheim, 1988.
(18) Song, O. K.; Wang, C. H.; Cho, B. R.; Je, J. T. *J. Phys. Chem.* **1995**, *99*, 6808.
(19) Duan, X.-M.; Konami, H.; Okada, S.; Oikawa, H.; Matsuda, H.; Nakanishi, H. *J. Phys. Chem.* **1996**, *100*, 17780.
(20) Kim, S.; Park, S. Y. *Mol. Cryst. Liq. Cryst.* **1999**, *337*, 405.
(21) Kim, S.; Park, S. Y. *Bull. Korean Chem. Soc.* **1999**, *20*, 473.
(22) Trollsås, M.; Hult, A.; Percec, V. *Macromol. Chem. Phys.* **1995**, *196*, 1821.
(23) Kim, S.; Park, S. Y. *Polym. Prepr.* **2000**, *41*, 804.
(24) Kim, S.; Moon, H.; Hwang, J.; Sohn, J.; Seo, J.; Park, S. Y.; Kang, T. I.; Cho, B. R. *Chem. Phys.* **2000**, *256*, 289.
(25) Schulman, S. G. *Fluorescence and Phosphorescence Spectroscopy: Physicochemical Principles and Practice*; Pergamon: Oxford, 1977; p 157.
(26) Rajalakshimi, N. In *Untra-Violet and Visible Spectroscopy. Chemical Applications*; Rao, C. N. R., Ed.; Butterworth: London, 1967; Chapter 10.
(27) Kasha, M.; Rawls, H. R.; El-Bayoumi, M. A. *Pure Appl. Chem.* **1965**, *11*, 371.
(28) Itaya, A.; Watanabe, K.; Imamura, T.; Miyasaka, H. *Thin Solid Films* **1997**, *292*, 204.
(29) Tazuke, S.; Winnik, M. A. In *Photophysical and Photochemical Tools in Polymer Science*; Winnik, M. A., Ed.; D. Reidel Publishing Company: Dordrecht, 1986; p 15.
(30) Tamai, Y.; Yamazaki, I.; Masuhara, H.; Mataga, N. *Chem. Phys. Lett.* **1984**, *104*, 485.

MA002087E